ϕ = volume fraction of suspended solids
$\bar{\epsilon}$ = energy dissipated per unit mass

LITERATURE CITED

Burke, F. P., "Assessment of Anti-Solvent Requirements for Wilsonville SRC Power Plant: Batch Studies," Conoco Coal Development Co. memorandum RM-14224 (Nov., 1976).

Gorin, E., C. J. Kulik, H. E. Lebowitz, "De-Ashing of Coal Liquefaction Products by Impartial Deasphalting I—Hydrogen Doner Extraction Effluents," *Ind. Eng. Chem. Proc. Des. Dev.*, **16**, 95 (1977).

Howarth, W. J., "Measurement of Coalescence Frequency in an Agitated Tank," *AIChE J.*, **13** (5), 1007-1013 (1967).

Huang, H., and J. Fischer, "Laboratory Studies for Separation of Solvents from Synthoil Gross Product," Argonne National Lab. Report ANL76-9 (1976).

Nagata, Shinji, "Mixing: Principles and Applications," Wiley & Sons, New York (1975).

Ondeyka, J. G., F. H. Verhoff, and J. D. Henry, "Indirect Measurement of Sedimentation Rates at High Temperature and Pressure by X-ray Photography," *Ind. Eng. Chem. Fundam.*, **17**, 217 (1978).

Rodger, W. A., V. G. Trice, Jr., and J. H. Rushton, "Fluid Motion Effect on Interfacial Area of Dispersions," *Chem. Eng. Prog.*, **52**, 515 (1956).

Rodgers, B. R., S. Katz and P. R. Westmoreland, "Supporting Research and Development on Separations Technology," Final Report ORNL/TM-58 43 (October, 1977).

Shinnar, R., and J. M. Church, "Predicting Particle Size in Agitated Dispersions," *Ind. Eng. Chem.*, **52**, 253 (1960).

Snell, G. J., and A. A. Simone, "The Application of the Lummus Anti-Solvent De-Ashing Technology to Solvent Refined Coal Solution," EPRI Report No. AF-234 (September, 1976).

Vermeulen, T., G. M. Williams, and G. E. Langlois, "Interfacial Area in Liquid-Liquid and Gas-Liquid Agitation," *Chem. Eng. Prog.*, **51**, 85 (1955).

Vold. M. J., "Computer Simulation of Floc Formation in a Colloidal Suspension," *J. Colloid Sci.*, **18**, 684-695 (1963).

Manuscript received May 1, 1978; revision received September 26, and accepted October 5, 1978.

Calculation of the Governing Equations for a Seriated Unequal Velocity, Equal Temperature Two-Phase Continuum

ROBERT W. LYCZKOWSKI

Lawrence Livermore Laboratory
Livermore, California

and

CHARLES W. SOLBRIG

EGG&G Idaho Inc.,
Idaho Falls, Idaho

The governing equations describing the flow of an unequal phase velocity, equal phase temperature (UVET) seriated two-phase continuum as derived by Solbrig and Hughes (1978) are solved in this article, in one space dimension. A simple implicit iterative solution procedure is developed to numerically evaluate the five non-linear coupled field equations. Analytical solutions are developed, against which the computer code results are compared. The prototype UVET code results are compared to the equivalent equal phase velocity, equal phase temperature (EVET) code results for the same problem. Major phenomena such as phase flow reversal, countercurrent flow and flooding-like behavior are predicted.

SCOPE

Our objectives are to develop a solution procedure for an unequal velocity, equal phase temperature seriated continuum, to compare the computed results against analytical solutions, and to predict *a priori*, major physical phenomena using the theory. The predictions of unequal velocity phase separation calculated here are of use in many aspects of energy analysis, including vertical pneumatic conveying, fluidized beds, and nuclear safety. The theoretical bases for the model were developed by Solbrig and Hughes (1978).

The theory requires separate continuity and momentum equations for each phase and a mixture energy equation. A seriated continuum is one which represents phase interaction expressions by differences of velocity, for example, rather than gradients. The model has the potential to describe far more phenomena than the equal velocity or gas dynamics model usually used.

Robert Lyczkowski is presently at The Institute of Gas Technology, Department of Gas Engineering, 3424 S. State St., Chicago, Illinois 60616, and is consultant for Lawrence Livermore Laboratory, Livermore, California. Charles Solbrig is presently at Commonwealth Edison Co., P.O. Box 767, Chicago, Illinois.

CONCLUSIONS AND SIGNIFICANCE

A simple implicit numerical procedure is developed to solve the governing equations describing a seriated unequal velocity, equal temperature two-phase continuum. It is demonstrated that these field equations predict quite naturally important physical phenomena, such as countercurrent flow and phase flow reversal and flooding-like behavior during a transient. Comparisons with analytical and simplified numerical solutions lend confidence to the predicted results. Comparison to equal velocity simulations of the same problem reveal that this simpler theory is incapable of properly predicting important phenomena.

The governing equations describing a general transient three-dimensional seriated continuum in thermodynamic equilibrium were derived by Solbrig and Hughes (1978). Included in that description are separate continuity and momentum equations for each phase, and a mixture energy equation and imbedded stationary surfaces, which might represent a nuclear reactor core or a porous medium. As explained by Solbrig and Hughes, a seriated continuum is distinguished from an interpenetrating continuum, for example, by the representation of interphase friction with velocity differences rather than velocity gradients. Sufficient constitutive relations are derived to mathematically close the equation set, so that the model is amenable to numerical computations.

The general formulation of the three-dimensional seriated continuum model is reduced in our work to a one-dimensional representation without an imbedded stationary solid. A simple implicit iterative numerical procedure is developed to solve the five resultant non-linear partial differential field equations. The behavior of the unequal phase velocity, equal phase temperature (UVET) two-phase flow model is investigated by solving several thought problems representing phase separation, countercurrent flow and flooding-like behavior. The computations show that such phenomena can be predicted. Several analytical solutions are obtained, against which the results are successfully compared. Some of the thought problems are compared with equivalent simulations using an equal phase velocity, equal phase temperature (EVET) or homogeneous equilibrium model (HEM). These comparisons demonstrate some inadequacies of the EVET or HEM model.

GOVERNING FIELD EQUATIONS

The one-dimensional constant area single phase and seriated continuum basic field equations are listed in this section in the forms ready for finite differencing. The appropriate equations of state are also listed.

Single Phase Flow

In the single phase (α_l or $\alpha_g = 0$) region, the governing equations are given by

Continuity:

$$\frac{\partial \rho_a}{\partial t} + \frac{\partial}{\partial x}(\rho_a v^a) = 0 \tag{1}$$

Momentum:

$$\frac{\partial}{\partial t}(\rho_a v^a) + \frac{\partial}{\partial x}(\rho_a v^a v^a) + \frac{\partial p}{\partial x} = -\overline{A}_{wa} B_{wa} v^a + \rho_a g_x \tag{2}$$

Energy:

$$\frac{\partial}{\partial t}[\rho_a(u_a + \tfrac{1}{2} v^a v^a)] + \frac{\partial}{\partial x}[\rho_a v^a (u_a + \tfrac{1}{2} v^a v^a)] + \frac{\partial}{\partial x}(p v^a) = q_w{}^a + \rho_a v^a g_x \tag{3}$$

The equation of state is given by

$$\rho_a = \rho_{aeos}(p, u_a) \tag{4}$$

Symbols are defined in the Notation section.

Seriated Continuum Model

The one-dimensional seriated continuum basic field equations are listed here, together with the appropriate equations of state.

Vapor Continuity:

$$\frac{\partial}{\partial t}(\alpha_g \rho_g) + \frac{\partial}{\partial x}(\alpha_g \rho_g v^g) = \dot{m} \tag{5}$$

Liquid Continuity:

$$\frac{\partial}{\partial t}(\alpha_l \rho_l) + \frac{\partial}{\partial x}(\alpha_l \rho_l v^l) = -\dot{m} \tag{6}$$

Vapor Momentum:

$$\frac{\partial}{\partial t}(\alpha_g \rho_g v^g) + \frac{\partial}{\partial x}(\alpha_g \rho_g v^g v^g) = -\alpha_g \frac{\partial p}{\partial x} + \hat{\dot{m}} v^g - \overline{A}_{gl} B_{gl}(v^g - v^l) - \overline{A}_{wg} B_{wg} v^g + \alpha_g \rho_g g_x \tag{7}$$

Liquid Momentum:

$$\frac{\partial}{\partial t}(\alpha_l \rho_l v^l) + \frac{\partial}{\partial x}(\alpha_l \rho_l v^l v^l) = -\alpha_l \frac{\partial p}{\partial x} - \hat{\dot{m}} v^l - \overline{A}_{gl} B_{gl}(v^l - v^g) - \overline{A}_{wl} B_{wl} v_x{}^l + \alpha_l \rho_l g_x \tag{8}$$

Mixture Energy:

$$\frac{\partial}{\partial t}(\rho u) + \frac{1}{2}\frac{\partial}{\partial t}(\alpha_g \rho_g v^g v^g + \alpha_l \rho_l v^l v^l) + \frac{\partial}{\partial x}\left[\alpha_g \rho_g v^g \left(u_g + \frac{1}{2} v^g v^g\right) + \alpha_l \rho_l v^l \left(u_l + \frac{1}{2} v^l v^l\right)\right] + \frac{\partial}{\partial x}[p(\alpha_l v^l + \alpha_g v^g)] = \overline{A}_{gl} B_{gl}(v^l - v^g)(v^{*g} - v^{*l}) + q_w + \rho v g_x \tag{9}$$

The second term on the right hand side of Equation (9) represents the sum of the work terms caused by interphase shear. Solbrig and Hughes (1978) argue that such terms cause no work. If the starred velocities in Equation (9) representing the characteristic velocity causing such work terms are set equal, the term disappears naturally. In our work, however, these characteristic velocities are taken to be the velocity of the opposite phase as

$$v^{*g} = v^l \tag{10}$$

and

$$v^{*l} = v^g \tag{11}$$

This work term was found to exert a negligible effect on the solutions generated here.

The field equations are coupled by the interaction terms which include the interphase friction force, $\bar{A}_{ab} B_{ab} (v^a - v^b)$ and the mass transfer rate, $\dot{m}$. The term $\hat{\dot{m}v^a}$ represents interphase momentum transfer associated with phase change. Models for $\hat{v^a}$ are given by Solbrig and Hughes (1978). The term is not used here.

Additional coupling enters through the constraint that the volume fractions add up as

$$\alpha_g + \alpha_l = 1 \tag{12}$$

There are five differential equations for the eight unknowns, ρ_g, ρ_l, α_g, v^l, v^g, u_l, and u_g. Therefore, in order to mathematically close the equation set, two equations of state are required, one for each phase as

$$\rho_a = \rho_{a_{eos}}(p) \quad a = l, g \tag{13a}$$

and

$$u_a = u_{a_{eos}}(p) \quad a = l, g \tag{13b}$$

which are representations of the properties of each phase. The system geometry, wall and interphase friction relations are assumed to be given. It is further assumed that the phase internal shears can be treated by using steady-state friction factor correlations for wall and interphase friction. These correlations, like the steady-state heat transfer correlations, are flow regime dependent. A complete prototype of correlations, based on micromodels, has been developed which can be used in conjunction with the two-fluid field equations, Solbrig et al. (1978), Hughes et al. (1976). Steady-state flow regime maps for both horizontal and vertical flow facilitate the selection of the proper correlations, Solbrig et al. (1978), Hughes et al. (1976). The average mixture quantities are given by

Density:

$$\rho = \alpha_l \rho_l + \alpha_g \rho_g \tag{14}$$

Velocity:

$$\rho v = \alpha_l \rho_l v^l + \alpha_g \rho_g v^g \tag{15}$$

Energy:

$$u = (\alpha_l \rho_l u_l + \alpha_g \rho_g u_g)/\rho \tag{16}$$

The equation system given above does not include the transient flow force or added mass terms. Omission of these terms is not considered to be detrimental to most applications of the two-fluid model.

General Pressure Field Equation

The so-called pressure field equation replaces the continuity equation in the single phase region and the liquid continuity equation in the two-phase region. The general pressure field equation is obtained by first differentiating the continuity equations, Equations (5) and 16), as

$$\frac{\partial^2}{\partial t^2}(\alpha_g \rho_g) + \frac{\partial^2}{\partial t \partial x}(\alpha_g \rho_g v^g) = \frac{\partial \dot{m}}{\partial t} \tag{17}$$

and

$$\frac{\partial^2}{\partial t^2}(\alpha_l \rho_l) + \frac{\partial^2}{\partial t \partial x}(\alpha_l \rho_l v^l) = -\frac{\partial \dot{m}}{\partial t} \tag{18}$$

Next, the phase momentum equations, Equations (7) and (8), are differentiated with respect to space as

$$\frac{\partial^2}{\partial x \partial t}(\rho_g \alpha_g v^g) + \frac{\partial^2}{\partial x^2}(\rho_g \alpha_g v^g v^g) + \frac{\partial}{\partial x}\left(\alpha_g \frac{\partial p}{\partial x}\right) + \frac{\partial}{\partial x}[\bar{A}_{gl} B_{gl}(v^g - v^l)] + \frac{\partial}{\partial x}(\bar{A}_{wg} B_{wg} v^g) = \frac{\partial}{\partial x}(\hat{\dot{m}v^g}) + g_x \frac{\partial \alpha_g \rho_g}{\partial x} \tag{19}$$

and

$$\frac{\partial^2}{\partial x \partial t}(\rho_l \alpha_l v^l) + \frac{\partial^2}{\partial x^2}(\rho_l \alpha_l v^l v^l) + \frac{\partial}{\partial x}\left(\alpha_l \frac{\partial p}{\partial x}\right) + \frac{\partial}{\partial x}[\bar{A}_{gl} B_{gl}(v^l - v^g)] + \frac{\partial}{\partial x}(\bar{A}_{wl} B_{wl} v^l) = -\frac{\partial}{\partial x}(\hat{\dot{m}v^l}) + g_x \frac{\partial(\alpha_l \rho_l)}{\partial x} \tag{20}$$

Assuming that the cross partial derivatives are equal as

$$\frac{\partial^2}{\partial t \partial x}(\alpha_g \rho_g v^g) = \frac{\partial^2}{\partial x \partial t}(\alpha_g \rho_g v^g) \tag{21}$$

and

$$\frac{\partial^2}{\partial t \partial x}(\alpha_l \rho_l v^l) = \frac{\partial^2}{\partial x \partial t}(\alpha_l \rho_l v^l) \tag{22}$$

and manipulation of Equations (17) through (20) produces the general pressure field equation as

$$\frac{\partial^2 \rho}{\partial t^2} = \frac{\partial^2}{\partial x^2}(\rho_l \alpha_l v^l v^l + \rho_g \alpha_g v^g v^g) + \frac{\partial^2 p}{\partial x^2} + \frac{\partial}{\partial x}(\bar{A}_{wl} B_{wl} v^l + \bar{A}_{wg} B_{wg} v^g) + \frac{\partial}{\partial x}[\dot{m}(\hat{v^l} - \hat{v^g})] - g_x \frac{\partial \rho}{\partial x} \tag{23}$$

Equation (23) is used in finite difference form given in the next section to obtain the pressure. Equation (23) reduces naturally to the single phase pressure field equation given by

$$\frac{\partial^2 \rho_a}{\partial t^2} = \frac{\partial^2}{\partial x^2}(\rho_a v^a v^a) + \frac{\partial^2 p}{\partial x^2} + \frac{\partial}{\partial x}(\bar{A}_{wa} B_{wa} v^a) - g_x \frac{\partial \rho_a}{\partial x} \tag{24}$$

when α_g or α_l are zero and $\dot{m} = 0$.

FINITE DIFFERENCE FORM OF THE GOVERNING FIELD EQUATIONS

The continuous forms of both the single phase and two-fluid field equations were given in the previous section. In this section, the finite difference approximations to these equations are given. These sets of non-linear algebraic equations without indication as to how the numerical inversion is to be performed are referred to here as the "time-step" finite difference form of the differential equations. The basic mesh layout for interior nodes is shown in Figure 1. This "staggered mesh" arrangement is typical of the MAC (Welch et al. 1966), SMAC (Amsden and Harlow 1970), YAQUI (Amsden and Hirt 1973), and SCORE (Wnek et al. 1975), for example, computer codes.

The fundamental variables pressure, p, phase energies, u_a, and the mass transfer rate, m, are computed and defined at the center of each node j. The description of a technique to solve for the pressure is given in the next section. The volume fractions and phase thermodynamics densities derived from these fundamental variables are also defined at the cell centers. These quantities are denoted by f_j, where f is a fundamental variable and j is a node

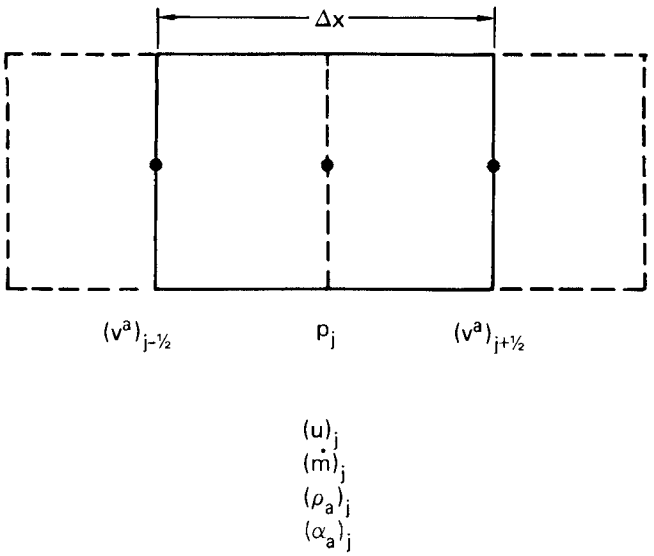

Figure 1. Interior finite difference mesh.

number. The phase velocities, v^l and v^g are computed and defined at the cell edges or junctions denoted by $j \pm ½$ for node j and denoted by $(v^a)_{j\pm1/2}$. The indices $j \pm ½$ are replaced inside the code by the integers j and $j + 1$ where j is a volume number. In the description which follows, when fundamental nodal values are needed at junctions they are linearly averaged. The same applies for junction velocities needed at cell centers.

The UVET computer code can begin computations in either the single phase liquid or vapor regimes. A phase may appear or disappear during the transient. When this situation occurs, the single-phase finite difference equations become singular because the determinants of both the temporal and spatial coefficient matrices become zero. The technique used to couple the single phase and two-fluid finite difference equations will be described later.

The basic form of the time-step difference equations is the fully implicit space centered difference scheme given here by

$$A_j^{n+1}\left(\frac{\vec{U}_i^{n+1}-\vec{U}_i^{n}}{\Delta t}\right)+B_j^{n+1}\left(\frac{\vec{U}_{j+1/2}^{m}-\vec{U}_{j-1/2}^{m}}{\Delta x}\right)=[F(\vec{U})]_j^m \quad (25)$$

where $\vec{U}$ is a vector of dependent variables. A and B are square coefficient matrices and F is a vector of sources and sinks. This scheme is shown to be unconditionally time-step stable with $F(\vec{U}) = 0$ for hyperbolic systems of differential equations (Lyczkowski et al. 1978). The space parts and the source and sink terms are differenced at time levels $m = n + 1$ and n. The seriated continuum time-step difference equations are given in this section. They are used at the cell centers and edges when two phases co-exist there. The single phase analogs of those equations result when $\alpha_g = 0$ or 1 ($\alpha_l = 1$ or 0) and $\dot{m} = 0$.

The continuity equations are differenced at the cell center j as

Vapor Continuity:

$$\frac{(\alpha_g\rho_g)_j^{n+1}-(\alpha_g\rho_g)_j^{n}}{\Delta t}+\frac{(\alpha_g\rho_g v^g)_{j+1/2}^{n+1}-(\alpha_g\rho_g v^a)_{j-1/2}^{n+1}}{\Delta x}=(\dot{m})_j^{n+1} \quad (26)$$

and

Liquid Continuity:

$$\frac{(\alpha_l\rho_l)_j^{n+1}-(\alpha_l\rho_l)_j^{n}}{\Delta t}+\frac{(\alpha_l\rho_l v^l)_{j+1/2}^{n+1}-(\alpha_l\rho_l v^l)_{j-1/2}^{n+1}}{\Delta x}=-(\dot{m})_j^{n+1} \quad (27)$$

Since the phase partial densities, $\alpha_a\rho_a$, are known only at cell centers, they are averaged at the cell edges, $j \pm ½$ as

$$(\alpha_a\rho_a)_{j\pm1/2}=\frac{(\alpha_a\rho_a)_j+(\alpha_a\rho_a)_{j\pm1}}{2} \quad (28)$$

The momentum equations are differenced at the cell edges $j \pm ½$ as

Vapor Momentum:

$$\frac{(\alpha_g\rho_g v^g)_{j+1/2}^{n+1}-(\alpha_g\rho_g v^g)_{j+1/2}^{n}}{\Delta t}+\frac{(\alpha_g\rho_g)_{j+1}^{n+1}(v^g v^g)_{j+1}^{n}-(\alpha_g\rho_g)_j^{n+1}(v^g v^g)_j^{n}}{\Delta x}$$
$$=-(\alpha_g)_{j+1/2}^{n+1}\frac{(p_{j+1}^{n+1}-p_j^{n+1})}{\Delta x}+\dot{m}_{j+1/2}^{n+1}(\hat{v^g})_{j+1/2}^{n+1}$$
$$-(\overline{A}_{gl}B_{gl})_{j+1/2}^{n}(v^g-v^l)_{j+1/2}^{n}$$
$$-(\overline{A}_{wg}B_{wg})_{j+1/2}^{n}(v^g)_{j+1/2}^{n}+(\alpha_g\rho_g)_{j+1/2}^{n+1}g_x \quad (29)$$

and

Liquid Momentum:

$$\frac{(\alpha_l\rho_l v^l)_{j+1/2}^{n+1}-(\alpha_l\rho_l)_{j+1/2}^{n}}{\Delta t}+\frac{(\alpha_l\rho_l)_{j+1}^{n+1}(v^l v^l)_{j+1}^{n}-(\alpha_l\rho_l)_j^{n+1}(v^l v^l)_j^{n}}{\Delta x}$$
$$=-(\alpha_l)_{j+1/2}^{n+1}\frac{(p_{j+1}^{n+1}-p_j^{n+1})}{\Delta x}-\dot{m}_{j+1/2}^{n+1}(\hat{v^l})_{j+1/2}^{n+1}$$
$$-(\overline{A}_{gl}B_{gl})_{j+1/2}^{n}(v^l-v^g)_{j+1/2}^{n}$$
$$-(\overline{A}_{wl}B_{wl})_{j+1/2}^{n}(v^l)_{j+1/2}^{n}+(\alpha_l\rho_l)_{j+1/2}^{n+1}g_x \quad (30)$$

The phase velocities at the cell centers are obtained using

$$(v^a)_k=\frac{(v^a)_{k+1/2}+(v^a)_{k-1/2}}{2} \quad (31)$$

with

$$k=j, j+1$$

since they are known only at cell edges.

Mixture Energy Equation:

$$\frac{1}{\Delta t}[(\rho u)_j^{n+1}-(\rho u)_j^{n}]+\frac{1}{2\Delta t}[(\rho_g\alpha_g v^g v^g+\rho_l\alpha_l v^l v^l)_j^{n+1}-(\rho_g\alpha_g v^g v^g+\rho_l\alpha_l v^l v^l)_j^{n}]$$

$$+\frac{1}{\Delta x}\left[(v^g\rho_g\alpha_g u_g + v^l\rho_l\alpha_l u_l)_{j+12}^{n+1} - (v^g\rho_g\alpha_g u_g\right.$$

$$\left. + v^l\rho_l\alpha_l u_l)_{j-1/2}^{n+1}\right] + \frac{1}{2}\frac{1}{\Delta x}\{[\rho_g\alpha_g v^g(v^g)^2$$

$$+ \rho_l\alpha_l v^l(v^l)^2]_{j+1/2}^{n+1} - [\rho_g\alpha_g v^g(v^g)^2 + \rho_l\alpha_l v^l(v^l)^2]_{j-1/2}^{n+1}\}$$

$$+\frac{1}{\Delta x}\{[p(\alpha_l v^l + \alpha_g v^g)]_{j+1/2}^{n+1} - [p(\alpha_l v^l + \alpha_g v^g)]_{j-1/2}^{n+1}\}$$

$$= [q_w + \overline{A}_{gl}B_{gl}(v^l - v^g)^2 + \rho v\, g_x]_j^{n+1} \quad (32)$$

Equation (32) reduces to the single phase energy finite difference equation when α_g or α_l are zero.

The seriated continuum liquid continuity, Equation (26), is replaced by the finite difference form of the pressure field equation. The seriated continuum pressure equation is obtained by summing the two continuity equations, (26) and (27), and eliminating the phase mass fluxes at $j \pm \frac{1}{2}$, using the finite differenced momentum equations given by Equations (29) and (30) and similarly differenced phase momentum equations at $j - \frac{1}{2}$. The resultant expression is given by

$$\frac{1}{\Delta t}\left\{\left(\frac{\rho_j^{n+1} - \rho_j^n}{\Delta t}\right) + \frac{1}{\Delta x}[(\rho v)_{j+1/2}^n - (\rho v)_{j-1/2}^n\right\}$$

$$= \frac{1}{(\Delta x)^2}[(\rho_l\alpha_l)_{j+1}^{n+1}(v^lv^l)_{j+1}^n - 2(\rho_l\alpha_l)_j^{n+1}(v^lv^l)_j^n$$

$$+ (\rho_l\alpha_l)_{j-1}^{n+1}(v^lv^l)_{j-1}^n] + \frac{1}{(\Delta x)^2}[(\rho_g\alpha_g)_{j+1}^{n+1}(v^gv^g)_{j+1}^n$$

$$- 2(\rho_g\alpha_g)_j^{n+1}(v^gv^g)_j^n + (\rho_g\alpha_g)_{j-1}^{n+1}(v^gv^g)_{j-1}^n]$$

$$+ \frac{1}{(\Delta x)^2}[p_{j+1}^{n+1} - 2p_j^{n+1} + p_{j-1}^{n+1}]$$

$$+ \frac{1}{\Delta x}[(\overline{A}_{wl}B_{wl}v^l + \overline{A}_{wg}B_{wg}v^g)_{j+1/2}^n$$

$$- (\overline{A}_{wl}B_{wl}v^l + \overline{A}_{wg}B_{wg}v^g)_{j-1/2}^n]$$

$$+ \frac{1}{\Delta x}[\dot{m}_{j+1/2}^n(\hat{v}^l - \hat{v}^g)_{j+1/2}^{n+1}$$

$$- \dot{m}_{j-1/2}^n(\hat{v}^l - \hat{v}^g)_{j-1/2}^{n+1}] - \frac{g_x}{\Delta x}(\rho_{j+1/2}^{n+1} - \rho_{j-1/2}^{n+1}) \quad (33)$$

A similar Poisson equation for pressure is used in the modified ICE procedure (Harlow and Amsdem 1971). Equation (33) reduces to the single phase pressure equation when α_l or α_g becomes zero and $\dot{m} = 0$. The single phase pressure equation replaces the continuity equation.

The mass transfer rate, $\dot{m}$, is computed from the vapor continuity equation according to

$$\Delta t(\dot{m})_{j+1/2}^{n+1} = (\rho_g\alpha_g)_{j+1/2}^{n+1} - (\rho_g\alpha_g)_{j+1/2}^n$$

$$+ \frac{\Delta t}{\Delta x}[(\rho_g\alpha_g v^g)_{j+1}^{n+1} - (\rho_g\alpha_g v^g)_j^{n+1}] \quad (34)$$

The phase fluid properties are computed from

$$(\rho_a)_j^{n+1} = \rho_{aeos}(p_j^{n+1}), \quad (35)$$

and

$$(u_a)_j^{n+1} = u_{aeos}(p_j^{n+1}) \quad (36)$$

Since the pressure equation replaces a continuity equation, the appropriate density is obtained from the equation of state as

$$(\rho_a)^{n+1} = \rho_{aeos}[p^{n+1}, u_a^{n+1}] \quad (37)$$

The vapor volume fraction can then be computed from

$$\alpha_g = \frac{\rho_l(u_l - u)}{(\rho_g - \rho_l)u - (\rho_g u_g - \rho_l u_l)} \quad (38)$$

The liquid volume fraction is obtained from

$$\alpha_l = 1 - \alpha_g \quad (39)$$

Assuming expressions or values are assigned for q_w, $\overline{A}_{wa}$, B_{wa}, $\overline{A}_{gl}$, B_{gl} and g_x, there are sufficient equations to compute all the dependent variables, given proper initial and boundary conditions.

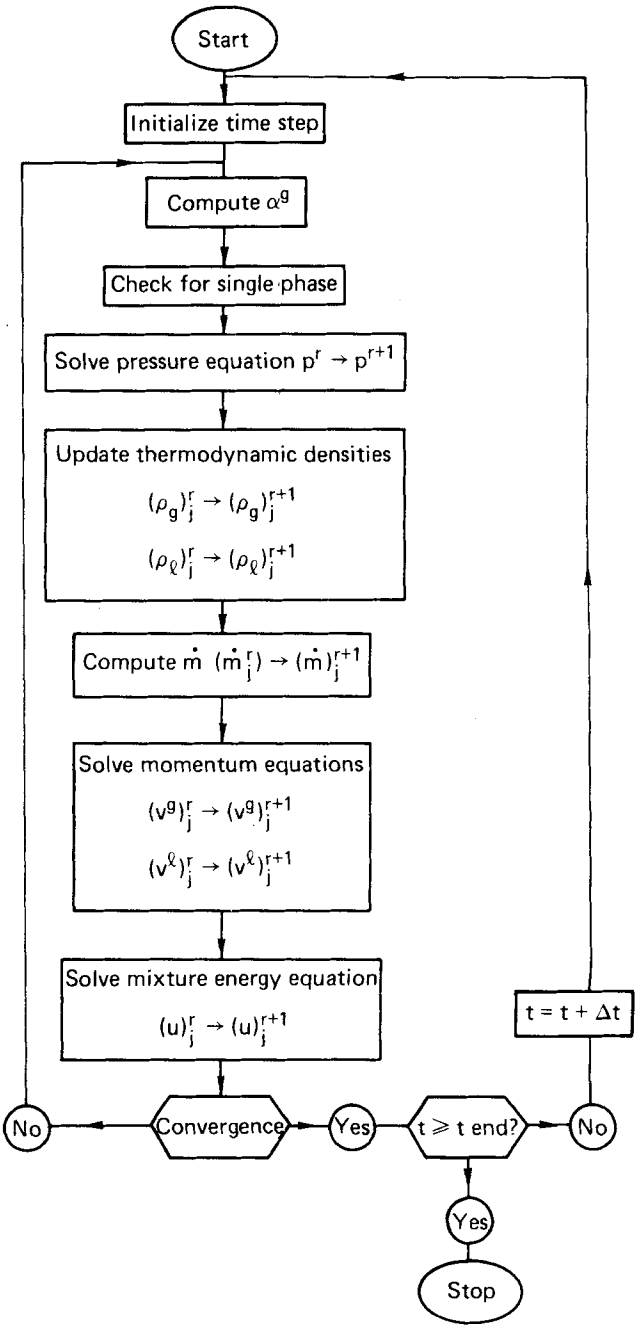

Figure 2. UVET code flow diagram.

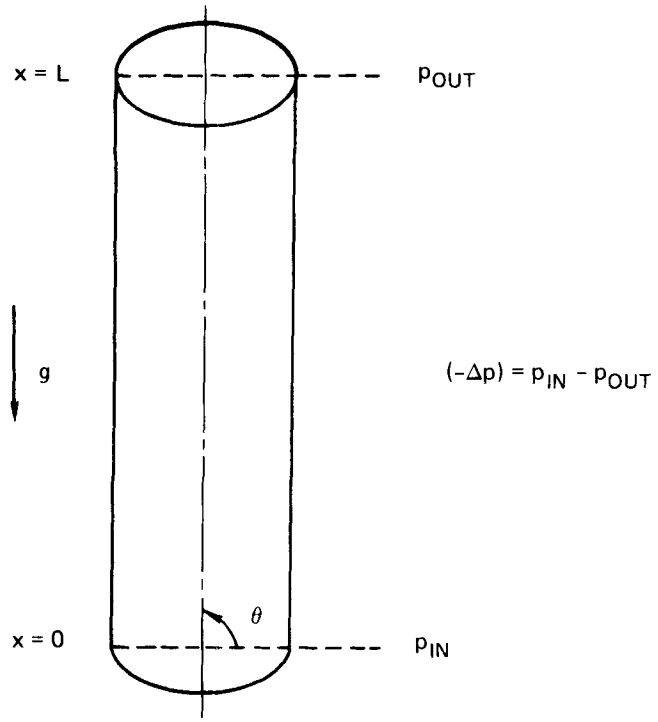

Figure 3. Pipe geometry.

ITERATIVE SOLUTION SCHEME

The solution sequence of the UVET-PF (pressure field) method is indicated in Figure 2. First the void fraction is computed. Depending on its value, either the single phase or seriated continuum equations are solved. The pressure equation is solved and used to update the thermodynamic properties and mass transfer. The momentum equations are solved, followed by the mixture energy equation. Convergence is checked using two successive pressure iterates as

$$R = \frac{p^{n+1,r+1} - p^{n+1,r}}{p^{n+1,r}} \leq \epsilon \qquad (40)$$

where $r + 1$ and r denote two successive iterates. When R is less than or equal to ϵ, convergence is assumed to occur and advancement to the next time step is performed.

BOUNDARY CONDITIONS

The boundary condition capability in the UVET-PF method has been maintained fairly simple. Specified pressure and energy are the only allowable boundary condition types.

Inflow Boundary

When fluid flows into the system at $x = 0$ shown in Figure 3, the pressure and energy states of the fluid are prescribed as

$$p(0, t) = p_{IN} \qquad (41)$$

and

$$u(0, t) = u_{IN} \qquad (42)$$

The numerical scheme used is second order correct in the space dimension while the field equations are only first order correct in space. Thus, more boundary conditions are required to solve the partial difference equations than are required to solve the partial differential equations. The additional conditions are referred to as extraneous boundary conditions. These are supplied in the UVET-PF numerical scheme, using simple linear extrapolation rather than those derived from the characteristic equations. The adequacy of using various boundary conditions was studied by Chu and Sereny (1974).

The inlet phase velocities are obtained from the two values of velocity next to the inlet junction as

$$v^a(0, t) = v^a(1) = \tfrac{1}{2}\,[3\,v^a(2) - v^a(3)] \qquad (43)$$

Equation (43) is obtained by averaging the imaginary point outside the pipe, $v^a(0)$ with the first node inside the pipe, $v^a(1)$, and eliminating the imaginary point outside the pipe by linear extrapolation from $v^a(2)$ and $v^a(3)$. Equation (43) is used for both single and two-phase flow conditions.

Outflow Boundary

When fluid flows out of the system at $x = L$ shown in Figure 2, the pressure is prescribed as

$$p(L, t) = p_{OUT} \qquad (44)$$

The velocity at $x = L$ is obtained using the difference equations, Equations (29) or (30) or both at $j + \tfrac{1}{2} = N + 1$, using an extrapolated value of pressure given by

$$p(N) = 2\,p_{OUT} - p(N - 1) \qquad (45)$$

where p_{OUT} is the prescribed value of pressure at $x = L$ and $p(N - 1)$ is the value of the pressure at the node next to the outlet junction.

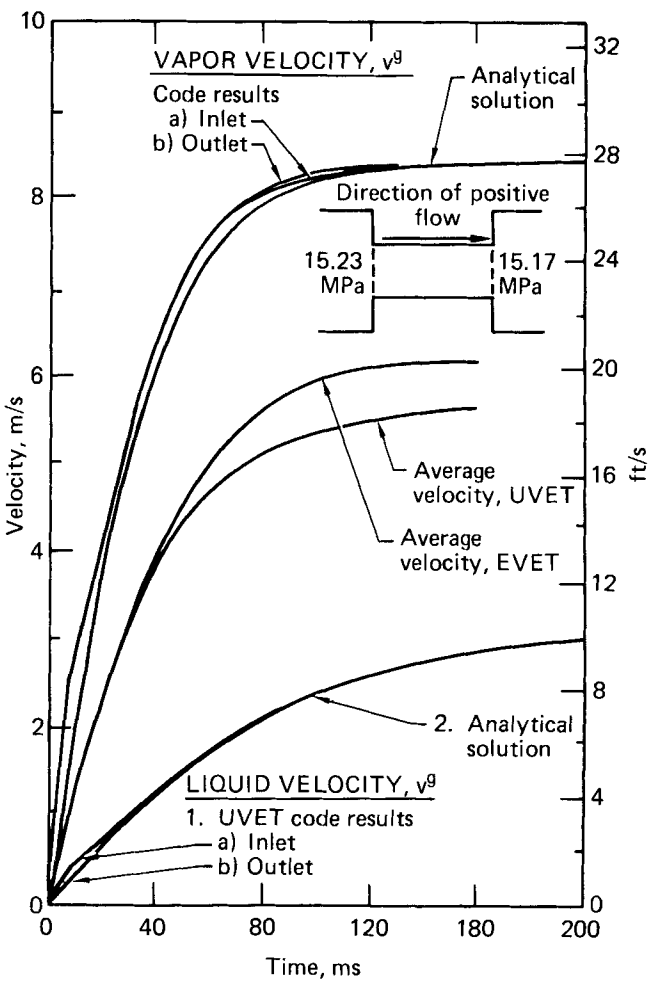

Figure 4. UVET code results and EVET code results, and simplified analytical solutions for a horizontal smooth tube. Initial pressure = 15.23 MPa, pipe length = 3.66 m, pipe diameter = 0.194 cm, energy = 2.02 MJ/kg$_m$, Δt = 10 ms, 9 volumes, $\overline{A}_{gl}B_{gl}$ = 16 kg/(m^3-s).

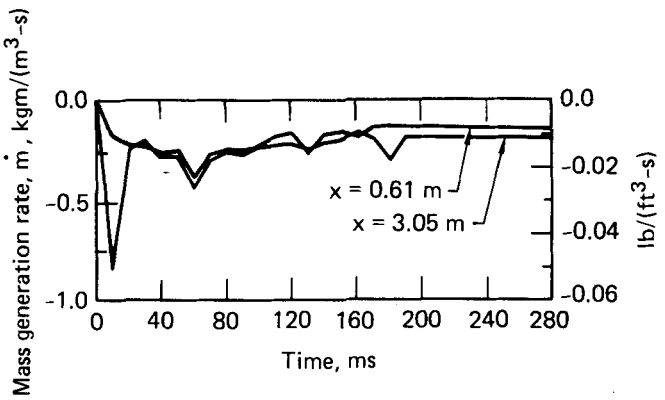

Figure 5. Vapor generation transient for horizontal smooth tube problems (refer to Figure 4).

The energy at $x = L$ is obtained by averaging an extrapolated value with the value known at the last node next to the junction as

$$u(L,t) = \tfrac{1}{2}[u(N-1) + 2\,u(N-1) - u(N-2)] \tag{46}$$

The value for the mass transfer rate, $\dot{m}$, is obtained in the same manner.

RESULTS OF COMPUTATIONS

The first problem chosen to test the UVET code is the acceleration of an initially motionless stratified mixture of steam and water, in a horizontal pipe, at uniform pressure and energy. The initial conditions are indicated in Figure 4. At time $t = 0^+$, two membranes at either end of the horizontal pipe are opened to reservoirs of constant pressure and energy.

An analytical solution exists for this problem, if certain assumptions are made. If the product of density times volume fraction, $\rho_a\alpha_a$ and mass transfer rate, $\dot{m}$, are negligible, the mass flow becomes a function of time alone as

$$\rho_a\alpha_a v^a = G^a(t) \tag{47}$$

Assuming that the kinetic energy, interphase friction and momentum transfer effects are negligible, the phase momentum equations may be written as

$$\frac{\partial G^a}{\partial t} + \alpha_a\frac{\partial p}{\partial x} + \frac{2\,f_{wa}\,|G^a|\,G^a}{\rho_a\alpha_a D} = 0 \tag{48}$$

where the product of $\overline{A}_{wa}\,\overline{B}_{wa}$ has been chosen to be

$$\overline{A}_{wa}\,B_{wa} = 2\,f_{wa}\,\rho_a\alpha_a\,|v^a|/D \tag{49}$$

Equation (49) may be integrated between $x = 0$ and $x = L$, assuming the friction factor is constant as

$$\frac{\partial G^a}{\partial t} + \frac{2\,f_{wa}\,|G^a|\,G^a}{\rho_a\alpha_a D} = \frac{\alpha_a(-\Delta p)}{L} \tag{50}$$

where $-\Delta p = p_{IN} - p_{OUT}$ is prescribed.

The solution to Equation (50) with $G^a = G_0{}^a$ at $t = 0$ is given by

$$v^a(t) = \left(\frac{(-\Delta p)\,D}{2\,L\,f_{wa}\rho_a}\right)^{1/2}\left[\frac{G_0{}^a + \tanh\,(t/t^*)}{1 + G_0{}^a\tanh\,(t/t^*)}\right] \tag{51}$$

where

$$(t^*)^{-1} = \left[\frac{2\,f_{wa}\,(-\Delta p)}{\rho_a\,D\,L}\right]^{1/2} \tag{51a}$$

Equation (51) was evaluated using the average steady-state UVFT computer code values of void fraction, densities, and friction factors as

$$v^l(t) = 3.124\tanh\,(10.13\,t), \quad \text{m/s} \tag{52}$$

and

$$v^g(t) = 8.409\tanh\,(22.70\,t), \quad \text{m/s} \tag{52a}$$

The results of the transient from the UVET code using virtually zero interfacial shear are compared with the analytical solutions in Figure 4. As can be seen, the code results during the transient agree quite well with the analytical solution. The agreement for the vapor velocity is not as good as for the liquid velocity since the assumption of incompressibility is not as valid. The average velocity is plotted and compared with an equivalent equal phase velocity (EVET) simulation of this problem. Even though the functional form of the wall friction is the same, the average flow for the unequal velocity calculation is lower than the equal velocity calculation. This trend is correct since the interphase friction is almost zero for the UVET simulation. As the product of $\overline{A}_{gl}B_{gl}$ is increased, the results of the two calculations for average velocity must become the same, as must the phase velocities.

Figure 5 shows the assumption of a negligible mass transfer rate is valid. The maximum value of the condensation rate is only 0.80 kg/(m³-s), which is negligible.

The steady-state velocities for the analytical solutions were forced to equal UVET code results. A more satisfactory approach to compare the UVET code results was arrived at by carrying out an independent integration of Equation (50) using the smooth tube Blasius friction factor expression given by (Knudsen and Katz 1958)

$$f_{wa} = 0.316\left(\frac{D|v^a|\rho_a}{\mu_a}\right)^{-1/4} \tag{53}$$

Equation (53) causes the simplified phase momentum equations to become

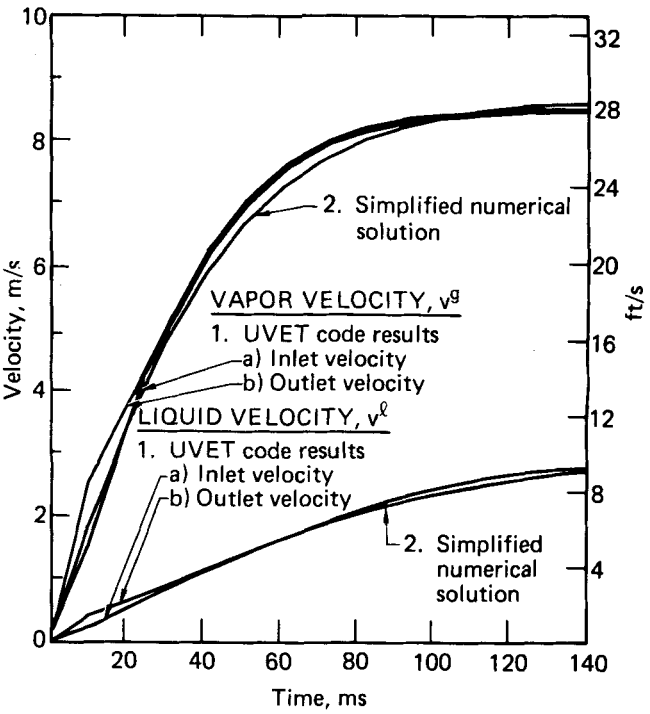

Figure 6. UVET results and simplified numerical solution for smooth tube using Blasius friction factor (same conditions as Figure 4).

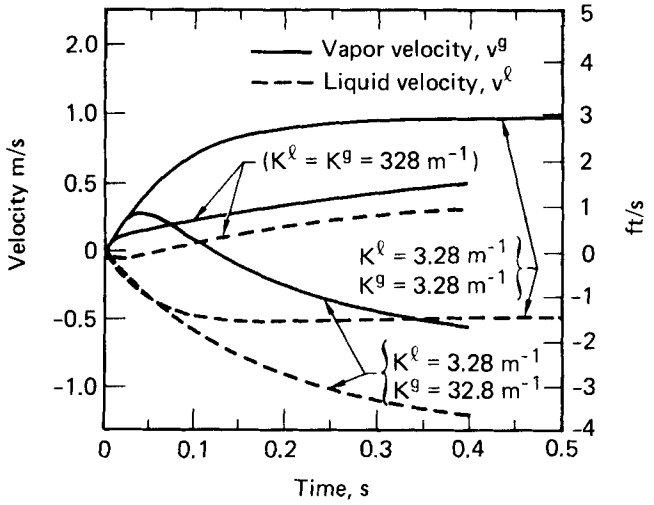

Figure 7. Simplified numerical solutions of Equation (54). p_{IN} = 15.237 MPa, p_{OUT} = 15.230 MPa, u = 2.02 MJ/kg$_m$.

$$\frac{dv^a}{dt} + 0.632\left(\frac{\mu_a}{\rho_a D^5}\right)^{1/4} |v^a|^{0.75} v^a = -\frac{\overline{A}_{gl}B_{gl}}{\alpha_a\rho_a}(v^a - v^b) + \frac{(-\Delta p)}{\rho_a L} - g\sin\theta \quad (54)$$

Equation (54) was integrated using a fourth order Runge-Kutta routine using $\overline{A}_{gl}B_{gl}$ = 16 kg/(m^3-s). The results are compared with the UVET code results in Figure 6. The agreement is quite satisfactory.

The ability of the seriated continuum theory to predict countercurrent flow and flow reversal in a vertical tube during a transient was investigated by numerically integrating Equation (54) using the Runge-Kutta method with the interphase friction of the functional form

$$\frac{\overline{A}_{gl}B_{gl}}{\alpha_a\rho_a} = K^a |v^a - v^b| \quad (55)$$

The phenomena of countercurrent flow and flow reversal during a transient were predicted and the results are presented in Figure 7.

When $K^l = K^g = 3.28\ m^{-1}$, both phases flow countercurrently for all times. The liquid equilibrates more slowly than the gas. When $K^l = 3.28\ m^{-1}$ and $K^g = 32.8\ m^{-1}$, the vapor initially moves upward but begins to be dragged

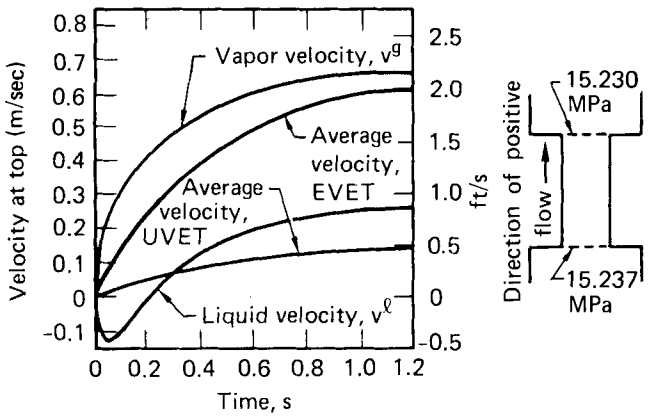

Figure 9. Liquid flow reversal in a smooth vertical pipe. Initial pressure = 15.237 MPa, pipe height = 3.65 m. pipe diameter = 6.194 cm, energy = 2.02 MJ/kg$_m$, Δt = 10 ms, 9 volumes, $\overline{A}_{gl}B_{gl}$ = 3.2 × 10^3 kg$_m$/(m^3-s).

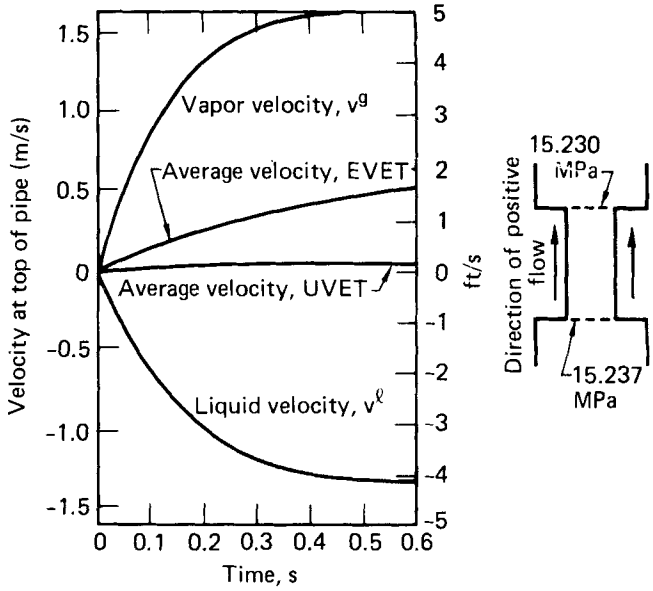

Figure 8. Countercurrent steam-water flow in a smooth vertical pipe. Initial pressure = 15.237 MPa, pipe height = 3.65 m, pipe diameter = 0.194 cm, energy = 2.02 MJ/kg$_m$, Δt = 10 ms, 9 volumes, $\overline{A}_{gl}B_{gl}$ = 16 kg$_m$/(m^3-s).

downward by the liquid. A ratio of 10 for K^g/K^l could mean that α_l is large compared to α_g and so the interpretation is plausible. This phenomenon might be called vapor phase flow reversal.

When $K^l = K^g = 328\ m^{-1}$, the liquid begins to flow downward, but reverses direction as it begins to be pulled upward by the vapor. This unity ratio of K^l/K^g could mean a smaller α_l, and so the interpretation is plausible. The phenomenon could be termed liquid phase flow reversal.

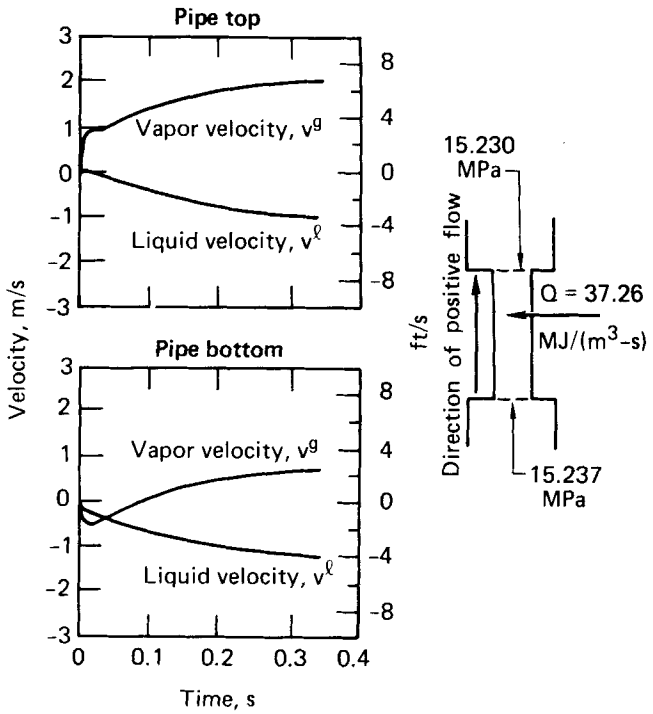

Figure 10. Effect of wall heat flux and prediction of flooding in a smooth vertical pipe. Initial pressure = 15.237 MPa, pipe height = 3.65 m, pipe diameter = 0.194 cm, energy = 2.02 MJ/kg$_m$, Δt = 10 ms, 9 volumes, $\overline{A}_{gl}B_{gl}$ = 16 kg$_m$/(m^3-s).

Now that the phenomena were predicted by the simple model, the next question is: Could the UVET code predict the phenomena? Figures 8 and 9 confirm that it did. Figure 8 shows the initiation of countercurrent flow from an initially motionless two-phase mixture in a vertical pipe. At $t = 0^+$, gravity is "turned on," and the pressure is reduced at the top. The vapor flows up, and because the initial condition was not at steady state and the interfacial shear is low, [$(\overline{A}_{gl}B_{gl} = 16$ kg/(m^3-s)], the water flows downward. This case corresponds approximately to the case $K_l = K_g = 3.28$ m^{-1} in Figure 7. The transient is not identical, but the order of magnitude of velocities is correct, and the trends are similar.

The average velocity obtained from an equivalent equal velocity simulation is compared with the average velocity obtained from the UVET simulation in Figure 8. The latter is considerably lower than the EVET simulation, which predicts both phases flowing co-currently upward at the same velocity.

In Figure 9, when $\overline{A}_{gl}B_{gl} = 3.2 \times 10^3$ kg/(m^3-s), liquid flow reversal is predicted. This case corresponds roughly to the curve for $K^l = K^g = 3.28$ m^{-1} in Figure 7. Once again, the trends are similar, even though actual values differ. But this, however, is not our purpose. We want to demonstrate that the code would predict important physical phenomena. If the simple model fails to predict the phenomena, it would be senseless to fish for them in the more complicated code. UVET and the EVET average velocities for this simulation are compared in Figure 9, where the high interphase friction has increased the UVET average velocity. But the EVET simulation did not predict any flow reversal.

The final study was to assess the effect of wall heat flux on the phase flow transients in a vertical pipe. The conditions are the same as for the initiating countercurrent flow with a step decrease in pressure at the top of a vertical pipe at $t = 0^+$ (shown in Figure 8). Except now, simultaneously, wall heat flux is "turned on." Immediately, the steam is expelled from both ends of the pipe(Figure 10). The water momentarily "floods" at the top of the pipe, in the sense that it remains motionless, momentarily. It falls downward at the bottom. Thus, the situation is predicted where countercurrent flow exists at the top and bottom of the pipe, but the phases are flowing in opposite directions. Flow reversal occurs in the spatial direction for both phases. The steam velocity at the top is higher than for the case of zero wall heat flux, and tends to hold the water up, or result in "flooding," which is predicted without any "flooding" correlation.

ACKNOWLEDGMENTS

The cooperation and programming assistance of G. A. Mortensen, R. E. Narum, C. Noble and W. J. Suitt are gratefully acknowledged. This work was performed while at the Idaho National Engineering Laboratory (INEL).

NOTATION

$\overline{A}_{gl}$ = surface area between vapor and liquid phase per unit volume
$\overline{A}_{wa}$ = surface area of phase "a" on contact with the wall per unit volume
B_{gl} = friction coefficient between vapor and liquid phases
B_{wa} = stationary form and viscous drag between wall and phase "a"
D = pipe diameter
f_{wa} = friction factor between phase "a" and the wall
G^a = mass flux of phase "a" $= \rho_a\alpha_a v^a$
g = gravitational constant
g_x = axial component of acceleration due to gravity
K^a = defined by Equation (55)
L = pipe length
$\dot{m}$ = mass transfer rate per unit volume
p = thermodynamic pressure
p_{IN}, p_{OUT} = prescribed inlet and outlet pressure
Δp = $-(p_{OUT} - p_{IN})$
q_w^a = heating rate at the wall to phase "a" per unit volume
t = time
Δt = time step size
u = average specific internal energy $= (\alpha_g\rho_g u_g + \alpha_l\rho_l u_l)/\rho$
u_{aeos} = equation of state for specific internal energy of phase "a"
u_a = specific internal energy of phase "a"
u_{IN} = prescribed inlet internal energy
v = average velocity $= (\alpha_g\rho_g v^g + \alpha_l\rho_l v^l)/\rho$
v_a = velocity of phase "a"
$\hat{v}^a$ = intrinsic velocity of phase "a"
x = spatial direction
Δx = spatial mesh size
α_a = volume fraction of prase "a" $(\alpha_l = 1 - \alpha_g)$
θ = angle of inclination measured from the horizontal
ρ = mixture density $= \alpha_g\rho_g + \alpha_l\rho_l$
ρ_{aeos} = equation of state for density phase of "a"
ρ_a = thermodynamic density of phase "a"

Subscripts and Superscripts

a = phase "a"
b = phase "b"
g = vapor phase
i = volume index
j = junction index
l = liquid phase
$n, n+1$ = value at time levels $n\Delta t$ and $(n+1)\Delta t$
o = initial value
$r, r+1$ = iterate levels at time level $n+1$

LITERATURE CITED

Amsden, A. A., and F. H. Harlow, "The SMAC Method," Los Alamos Scientific Laboratory, LA-4370 (1970).

Amsden, A. A., and C. W. Hirt, "YAQUI: An Arbitrary Lagrangian-Eulerian Computer Program for Fluid Flow at All Speeds," Los Alamos Scientific Laboratory, LA-5100 (1973).

Chu, C. K., and Aron Sereny, "Boundary Conditions in Finite Difference Fluid Dynamic Codes," *J. Comp. Phys.*, **15**, 476-491 (1974).

Harlow, F. H., and A. A. Amsden, "A Numerical Fluid Dynamics Calculation Method for All Flow Speeds," *J. Comp. Phys.*, 8, 197-213 (1971).

Hughes, E. D., R. W. Lyczkowski, and J. H. McFadden, "An Evaluation of State-of-the-Art Two-Velocity Two-Phase Flow Models and Their Applicability to Nuclear Reactor Transient Analysis Volume 2: Theoretical Bases," Electric Power Research Institute NP-143 (Feb. 1976).

Knudsen, J. G., and D. L. Katz, *Fluid Dynamics and Heat Transfer*, McGraw-Hill, New York (1958).

Lyczkowski, R. W., D. Gidaspow, C. W. Solbrig, and E. D. Hughes, "Characteristics and Stability Analyses of Transient One-Dimensional Two-Phase Flow Equations and Their Finite Difference Approximations," *Nucl. Sci. Eng.*, **66**, 378-396 (1978).

Solbrig, C. W., and E. D. Hughes, "Governing Equations for a Seriated Continuum: An Unequal Velocity Model for Two-Phase Flow," in *Two-Phase Transport and Reactor Safety*, vol. I, pp. 307-362, Hemisphere Publ. Corp., Washington (1978).

Solbrig, C. W., J. H. McFadden, R. W. Lyczkowski, and E. D. Hughes, "Heat Transfer and Friction Correlations Required to Describe Steam-Water Behavior in Nuclear Safety Studies," pp. 100-128 in *Heat Transfer Research and Application*, AIChE, N.Y. (1978).

Welch, J. E., F. H. Harlow, J. P. Shannon, and B. J. Daly, "The MAC Method," Los Alamos Scientific Laboratory, LA-3425 (1966).

Wnek, W. J., J. D. Ramshaw, J. A. Trapp, E. D. Hughes, and C. W. Solbrig, "Transient Three-Dimensional Thermal-Hydraulic Analysis of Nuclear Reactor Fuel Rod Arrays: General Equations and Numerical Scheme," Aerojet Nuclear Co., ANCR-1207 (November, 1975).

Manuscript received August 8, 1977; revision received May 2, and accepted July 6, 1979.

Structural Analysis of Multicomponent Reaction Models:

Part I. Systematic Editing of Kinetic and Thermodynamic Values

JAN P. SØRENSEN

and

WARREN E. STEWART

Department of Chemical Engineering
University of Wisconsin
Madison, Wisconsin 53706

The consistency of a chemical reaction scheme depends in part on the numerical values given for its kinetic and thermodynamic constants. Part 1 of the present two-part treatment provides 1) a systematic procedure to reduce the given values to a self-consistent form, and 2) a proper selection of parameters whenever the values are to be improved by a subsequent regression analysis. Various completeness and consistency tests are described, including a search for illegal reaction loops arising from assumptions of irreversibility. The procedure is implemented on a computer and is illustrated with two examples.

SCOPE

The purpose of this article is to demonstrate a systematic procedure for analyzing a given reaction network and the proposed kinetic and thermodynamic values. This procedure includes consistency tests, which should be performed when several data sources are available, or when any of the reactions are treated as irreversible. It includes completeness tests, to determine whether additional kinetic and thermodynamic values are required. It includes the construction of a consistent set of kinetic and thermodynamic values from the raw data. Finally, there is a selection of adjustable parameters among the kinetic and thermodynamic variables, to allow adjustment of the model to fit additional data from reactor experiments.

It should be noted that the present analysis is not concerned with selecting a reaction network, but rather with testing the consistency of a given network. Nor is any attempt made to combine several inconsistent data in a least-squares sense; that can be done in a subsequent regression. The present procedure selects a subset of the proposed kinetic and thermodynamic values, and compares any redundant values with the solution thus obtained.

CONCLUSIONS AND SIGNIFICANCE

We provide a systematic procedure for editing raw kinetic and thermodynamic coefficients in multicomponent reaction models. The procedure includes several completeness and consistency tests, as well as compact parameterization when the model is to be improved by regression of additional data. The procedure also relieves the engineer of the tedious kinetic and thermodynamic calculations required to bring raw literature values into consistent form. It is particularly useful for large reaction networks, or when values from several sources are to be combined. For example, in the *n*-butane pyrolysis model given by Blakemore and Corcoran (1969), our procedure shows that the initiating reaction (1) should be considered reversible for consistency with the other reactions given.

Correspondence concerning this paper should be addressed to W. E. Stewart.

0001-1541-80-3085-0098-$00.85.